Simulation of the Active Corrector of Power Factor as a Means of Improving the Electromagnetic Compatibility and Energy Efficiency of Electric Locomotive's Auxiliary Electric Drive

Anatoliy Lavrentyev and Mikhail Pustovetov *

Posted Date: 23 May 2024

doi: 10.20944/preprints202405.1572.v1

Keywords: power factor active correction; cascaded loops control; AC electric locomotive; auxiliary electric drive; current control loop; voltage control loop; energy saving; electromagnetic compatibility

 doi:10.20944/preprints202405.1572.v1

Article

Simulation of the Active Corrector of Power Factor as a Means of Improving the Electromagnetic Compatibility and Energy Efficiency of Electric Locomotive's Auxiliary Electric Drive

Anatoliy Lavrentyev and Mikhail Pustovetov *

Department of Electrical and Electronics Engineering, Faculty of Automation, Mechatronics and Control, Don State Technical University, sq. Gagarin 1, 344000 Rostov-on-Don, Russia; spu-37.5@donstu.ru
* Correspondence: mgsn2006@yandex.ru

Abstract: The object of study in the article is the auxiliary variable-frequency electric drive onboard of an AC electric locomotive, and more precisely, the structure and parameters of the control system of the active corrector of power factor (ACPF), which is part of the electric drive, as a unit that ensures electromagnetic compatibility of the electric drive with other equipment on board the electric locomotive and catenary and its energy efficiency. The topic of the article's research is the substantiation of the structure of the ACPF control system, the choice of types (transfer functions) of controllers and the calculation of their parameters. The research method chosen was the calculation of the transfer functions of the controllers of the cascaded loops control system, followed by computer simulation using the OrCAD software. The results of simulating a cascaded two loops control system of an ACPF with different types of controllers are presented and analytically compared. It is concluded that it is advisable to use a cascaded two loops control system, containing a voltage control loop and a current control loop. The best results show the simulation when using an aperiodic current controller (A-controller) and a proportional-integral voltage controller (PI-controller). The data obtained serve as the basis for further improvement of the operation of the ACPF by enhancing and optimizing the settings, structure and algorithms of the control system, which, with the selected hardware of power converter unit, will allow the ACPF to perform its functions with a high degree of reliability in an entire range of disturbing and control influences.

Keywords: power factor active correction; cascaded loops control; AC electric locomotive; auxiliary electric drive; current control loop; voltage control loop; energy saving; electromagnetic compatibility

1. Introduction

As part of a modern AC electric drive, many devices are used that increase electromagnetic compatibility and energy efficiency such as: dv/dt filters [1,2], sine-wave filters [3,4], AC line reactors [5,6]. ACPF is one of the important elements of the power supply unit for auxiliary circuits of electric locomotives, as it promotes energy saving by reducing reactive power consumption and distortion power [7]. The circuits and operating principle of an ACPF are given in [7–11]. An example is the usage of ACPF based on a step-up (boost) DC-DC voltage pulse converter [7] as part of the PSN-169 auxiliary converter on board an EP200 type passenger AC electric locomotive manufactured in Russia. An alternative technical solution with similar functions is the use of a four-quadrant converter as part of an auxiliary electric drive [12–17]. In Figure 1 we can see an electrical circuit diagram and functional diagram of the electric locomotive's ACPF control system. In Figure 1 the following designations are adopted:

LPF – low pass filter;
RG – ramp generator;
VC – voltage controller;

Preprints.org (www.preprints.org) | NOT PEER-REVIEWED | Posted: 23 May 2024 doi:10.20944/preprints202405.1572.v1

CC – current controller;

TVG – triangular voltage generator;

NE – nonlinear element;

SSPC – setter of the shape (sinusoid) and phase of the AC input current i_c; let us note that in a real ACPF (not in a mathematical model, where we know a priori the phase of the input voltage v_c), synchronization of the operation of the SSPC with the frequency and phase of the input voltage is required, which is a separate task not considered in this article;

CS – rectified current i_d sensor;

VS – load DC voltage v_d sensor;

$V_{control\max}$ – the highest DC control voltage value;

$f_{carrier} = 1500$ Hz – carrier frequency of pulse-width voltage control (PWVC);

$MC_{\max}$ – the highest value of the modulation coefficient;

C_d – DC-link capacitor;

L_{rf}, C_{rf}, R_{rf} – elements of a resonant filter tuned to the frequency of 100 Hz (doubled catenary frequency);

$v_{reference}$ – control system reference voltage;

$\Delta\varphi$ – specified phase shift of the input current relative to the input voltage.

R_{load} – load impedance (the auxiliary load powered from the ACPF onboard of the electric locomotive EP200 is described in more detail in [18]).

L_c, R_c – input wires' parameters.

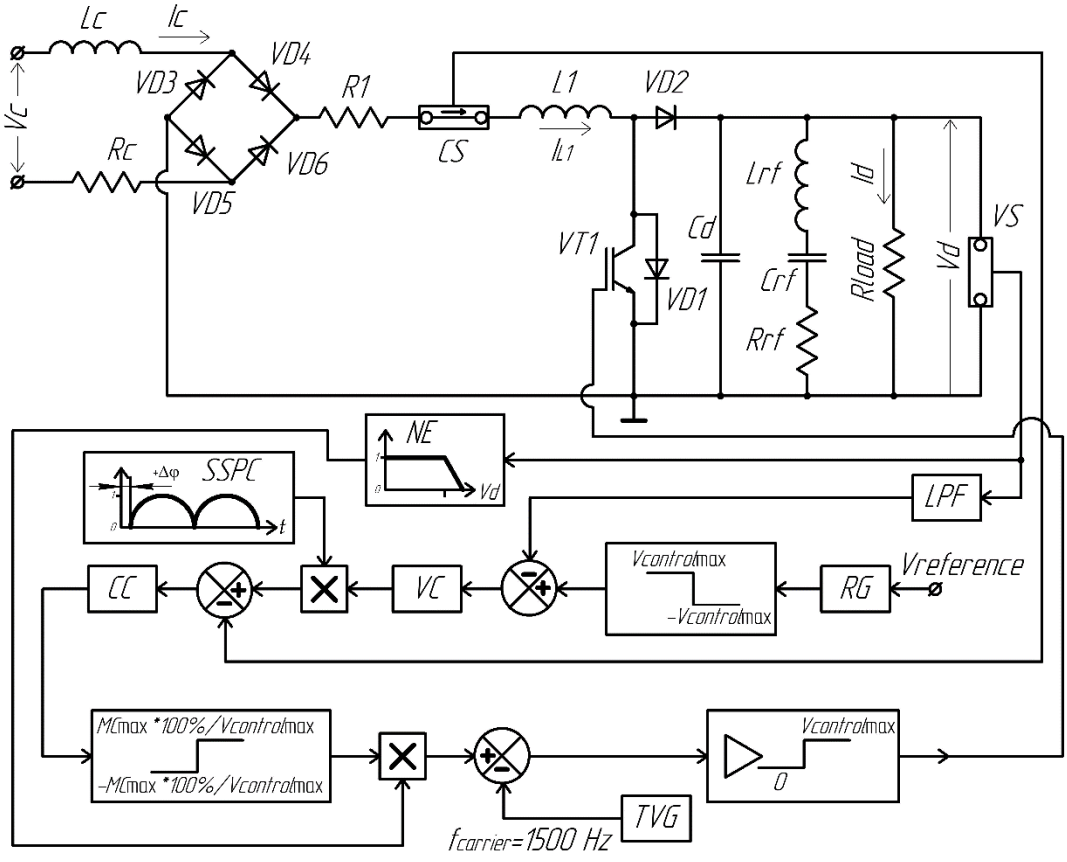

Figure 1. Electrical circuit diagram and functional diagram of the ACPF control system of the auxiliary electric drive of an electric locomotive.

 doi:10.20944/preprints202405.1572.v1

The main goals of ACPF control:

1) stabilization of the output DC voltage v_d at the load;

2) stabilization of DC load current i_d;

3) formation of a sinusoidal shape of the input AC current i_c;

4) ensuring a given phase shift (as a rule, no phase shift is required) of the AC input current i_c relative to the AC input voltage v_c.

Control goals 3 and 4 directly serve to correct (closer to unity) the power factor, that is, serve to improvement of the electromagnetic compatibility and energy efficiency of the auxiliary electric drive of an electric locomotive by reducing reactive power and distortion power. In [19] the definition of the power factor of an electrical equipment is given. Without retelling it verbatim, it can be noted that in the general case we mean sinusoidal voltage v_c and non-sinusoidal current i_c consumed by an electrical equipment. The power factor will be closer to unity, firstly, the smaller the phase shift of the fundamental harmonic of the AC input current from the AC input voltage, and secondly, the less distorted the input current i_c shape is (the closer it is to a pure sinusoid).

Control goals 2 and 3 can be combined into one goal, which is formulated as follows: the formation of a rectified current of a given amplitude through the input inductance L_1 of the ACPF, which has the shape of a rectified sinusoid vs time.

Assuming the input AC voltage of the ACPF $v_c = V_{cm}\sin(\omega t)$, in the case of in-phase input AC voltage and AC current, we will use the equation (1) to describe the current through the input inductance of the ACPF [7]:

$$i_{L1} = \frac{V_{cm}}{R_e} \cdot \left|\sin(\omega t)\right|, \qquad (1)$$

where is R_e - the equivalent input impedance of the ACPF.

Rectified current i_{L1} is a variable dependent on v_d, since load DC current i_d, representing the component of i_{L1}, is a variable dependent on v_d. The voltage v_d is generated as a result of pulsed control of the DC voltage by a transistor converter, namely as a result of switching the transistor VT1. This logical chain allows us to determine the number and hierarchy of coordinate control loops, as well as plants [20,21] in the loops.

2. Materials and Methods

Two control loops are required. The internal (slave) control loop is the current i_{L1} control loop. The external one will be the voltage v_d control loop. The plant in the current control loop is inductance L_1 - it is through it that it is necessary to ensure the current of a given shape and magnitude. The transfer function (TF) of the plant in the current loop is $W_{plant\_i}(s) = \frac{1}{L_1 \cdot s}$. The TF of the plant in the voltage control loop is a serial connection of the TF of the closed current i_{L1} control loop (denoted as $W_{closed\_i}(s)$) and the TF of the transistor converter (chopper) $W_{ch}(s)$.

Let us determine the type (TF) of the controller in the current control loop $W_{controller\_i}(s)$, using modulus optimum method. The desired TF of an open current control loop has the form of expression (2) [22] or expression (3):

 doi:10.20944/preprints202405.1572.v1

$$W_{open\_desired\_i}(s) = \frac{1}{a_i \cdot T_\mu \cdot s(T_\mu \cdot s + 1)}, \quad (2)$$

where T_μ is the small uncompensated time constant in the current circuit; $a_i = \frac{T_{0i}}{T_\mu}$ – ratio of time constants; T_{0i} – time constant of the optimized current control loop.

$$W_{open\_desired\_i}(s) = k_{si} \cdot W_{plant\_i}(s) \cdot W_{controller\_i}(s) = k_{si} \cdot \frac{1}{L_1 \cdot s} \cdot W_{controller\_i}(s), \quad (3)$$

where k_{si} is the TF of the current i_{L1} sensor.

$$k_{si} = \frac{V_{control\max}}{I_{L1\max}}, \quad (4)$$

where $I_{L1\max}$ is the greatest value of the current through the input inductance L_1 of the ACPF.

From (3) we express the TF of the current controller:

$$W_{controller\_i}(s) = \frac{W_{open\_desired\_i}(s)}{k_{si} \cdot W_{plant\_i}(s)} = \frac{\frac{1}{a_i \cdot T_\mu \cdot s \cdot (T_\mu \cdot s + 1)}}{k_{si} \cdot \frac{1}{L_1 \cdot s}} = \frac{L_1}{k_{si} \cdot a_i \cdot T_\mu} \left(\frac{1}{T_\mu \cdot s + 1} \right) =$$

$$= k_{controller\_i} \left(\frac{1}{T_{controller\_i} \cdot s + 1} \right), \quad (5)$$

where $k_{controller\_i} = \frac{L_1}{k_{si} \cdot a_i \cdot T_\mu}$ is the gain of the current controller; $T_{controller\_i} = T_\mu$ – time constant of the current controller.

Based on the form of the resulting expression (5), we can conclude that the TF of an aperiodic controller (A-controller) has been obtained, which can be represented as an operational amplifier (op-amp), covered by a feedback loop containing R and C connected in parallel. The standard approach to determining the TF of active correcting units based on an op-amp, set out in particular in [23], states that the TF of the active correcting unit in the case of a non-inverting op-amp:

$$W_a(p) = \frac{Z_2(p)}{Z_1(p)}, \quad (6)$$

where Z_1 is the impedance at the input of the correcting unit in the longitudinal branch; Z_2 – feedback impedance surrounding the op-amp. In relation to the A-controller, we obtain: $Z_1 = R_1$; $\frac{1}{Z_2} = \frac{1}{R_{feedback}} + \frac{1}{\frac{1}{s \cdot C_{feedback}}}$, where $Z_2 = \frac{R_{feedback}}{s \cdot C_{feedback} \cdot R_{feedback} + 1}$. The TF of the A-controller will be obtained in the form:

From (3) we express the TF of the current controller:

 doi:10.20944/preprints202405.1572.v1

$$W_{\text{Acontroller}}(s)=\frac{R_{feedback}}{R_1}\cdot\left(\frac{1}{C_{feedback}\cdot R_{feedback}\cdot s+1}\right)=k_{\text{A}}\cdot\left(\frac{1}{T_{\text{A}}\cdot s+1}\right). \quad (7)$$

Let's determine the type of controller in the voltage control loop $W_{controller\_v}(s)$. The desired TF of an open voltage control loop has the form of expression (8) [22] or (9):

$$W_{open\_desired\_v}(s)=\frac{1}{a_v\cdot a_i\cdot T_{\mu}\cdot s\cdot(a_i\cdot T_{\mu}\cdot s+1)}, \quad (8)$$

where $a_v=\frac{T_{0v}}{T_{0i}}$ is the ratio of time constants; T_{0v} – time constant of the optimized voltage control loop.

On the other side,

$$W_{open\_desired\_v}(s)=k_{sv}\cdot W_{closed\_i}(s)\cdot W_{ch}(s)\cdot W_{controller\_u}(s), \quad (9)$$

where k_{sv} is the TF of the voltage u_d sensor.

$$W_{closed\_i}(s)=\frac{1}{a_i\cdot T_{\mu}\cdot s\cdot(T_{\mu}\cdot s+1)+1}\cdot\frac{1}{k_{si}}\approx\frac{1/k_{si}}{a_i\cdot T_{\mu}\cdot s+1}, \quad (10)$$

$$W_{ch}(s)=\frac{k_{ch}}{T_{ch}\cdot s+1}. \quad (11)$$

According to [24], for transistor converters the time constant

$$T_{ch}=\frac{1}{f_s}, \quad (12)$$

Where $f_s\approx f_{carrier}$ is the switching frequency of transistor switch VT1.

Transistor converter gain

$$k_{ch}=\frac{V_{d\ rated}}{V_{control\max}}, \quad (13)$$

where $V_{d\ rated}$ is the rated value of the DC voltage at the load.

$$k_{sv}=\frac{V_{control\max}}{V_{d\ rated}}. \quad (14)$$

Let us rewrite (9) taking into account (10) and (11):

$$W_{open\_desired\_v}(s)=k_{sv}\cdot\frac{1/k_{si}}{a_i\cdot T_{\mu}\cdot s+1}\cdot\frac{k_{ch}}{T_{ch}\cdot s+1}\cdot W_{controller\_v}(s). \quad (15)$$

From (9) taking into account (15) we express the TF of the voltage controller:

Preprints.org (www.preprints.org) | NOT PEER-REVIEWED | Posted: 23 May 2024 doi:10.20944/preprints202405.1572.v1

$$W_{controller\_v}(s)=\frac{W_{open\_desired\_v}(s)}{k_{sv}\cdot W_{closed\_i}(s)\cdot W_{ch}(s)}=$$

$$=\frac{1}{\frac{a_v\cdot a_i\cdot T_\mu\cdot s\cdot(a_i\cdot T_\mu\cdot s+1)}{k_{sv}\cdot\frac{1/k_{si}}{a_i\cdot T_\mu\cdot s+1}\cdot\frac{k_{ch}}{T_{ch}\cdot s+1}}}=\frac{k_{si}}{a_v\cdot a_i\cdot k_{ch}\cdot k_{sv}}\cdot\left(\frac{T_{ch}}{T_\mu}+\frac{1}{T_\mu\cdot s}\right)=$$

$$=\frac{k_{si}}{a_v\cdot a_i\cdot k_{ch}\cdot k_{sv}}\cdot\frac{T_{ch}}{T_\mu}\cdot\left(1+\frac{1}{T_{ch}\cdot s}\right)=k_{controller\_v}\cdot\left(1+\frac{1}{T_{controller\_v}\cdot s}\right) \quad (16)$$

where $k_{controller\_v}=\frac{k_{si}}{a_v\cdot a_i\cdot k_{ch}\cdot k_{sv}}\cdot\frac{T_{ch}}{T_\mu}$ is the gain of the voltage controller; $T_{controller\_v}=T_{ch}$ – time constant of the voltage controller.

From expression (16) it follows that the TF of the proportional-integral controller (PI-controller) has been obtained. Setting up the control loops is thus reduced to choosing the values T_μ, a_i, a_v and $I_{L1\max}$.

Let's take into account that the additional goals of regulating cash registers are:

1) limitation of the voltage duty cycle (modulation factor) at the PWVC of the transistor switch VT1 (for example, $MC_{\max}=0.85$);

2) limiting the maximum instantaneous voltage $v_{d\max}$ (for example, $v_{d\max}=700$ V) - for this, the circuit in Figure 1 containing an additional channel for direct limitation of the output voltage (see NE in Figure 1). The action of this channel is based on the fact that when $v_{d\max}=700$ V is reached, the signal about this, bypassing the regulators, blocks the unlocking of the transistor switch until the output voltage decreases;

3) the ability to maintain the shape of the mains current close to sinusoidal when the load at the ACPF output changes.

3. Results

Computer simulation by means of OrCAD shows that a good setting option is the following combination of parameters:

$a_i=a_v=4$; $T_\mu=0.1\cdot T_{ch}$; $I_{L1\max}=650$ A.

In this case, other parameters of the ACPF control system have the following values:

$L_1=0.78\cdot10^{-3}$ H; $k_{ch}=\frac{V_{d\ rated}}{V_{control\_\max}}=\frac{660}{10}=66$ V/V;

$k_{si}=\frac{V_{control\max}}{I_{L1\max}}=\frac{10}{650}=0.0153$ V/A;

$k_{sv}=\frac{V_{control\max}}{V_{d\ rated}}=\frac{10}{660}=0.0152$ V/V;

$T_{controller\_i}=T_\mu=0.1\cdot T_{ch}=0.1\cdot0.00067\approx0.00007$ s;

Preprints.org (www.preprints.org) | NOT PEER-REVIEWED | Posted: 23 May 2024 doi:10.20944/preprints202405.1572.v1

$$k_{controller\_i} = \frac{L_1}{k_{si} \cdot a_i \cdot T_\mu} = \frac{0.78 \cdot 10^{-3}}{0.0153 \cdot 4 \cdot 0.00007} = 182.1;$$

$$T_{controller\_v} = T_{ch} = \frac{1}{f_s} = \frac{1}{1500} = 0.00067 \text{ s.}$$

$$k_{controller\_v} = \frac{k_{si}}{a_v \cdot a_i \cdot k_{ch} \cdot k_{sv}} \cdot \frac{T_{ch}}{T_\mu} = \frac{0.0153}{4 \cdot 4 \cdot 66 \cdot 0.0152} \cdot \frac{0.00067}{0.00007} = 0.0092.$$

These settings are preferred if the load resistance can vary widely. The simulation results for $R_{load\_rated} = 3.94$ Ohm (corresponding to a converter power of about 110 kVA) we can see in Figure 2 and Figure 3.

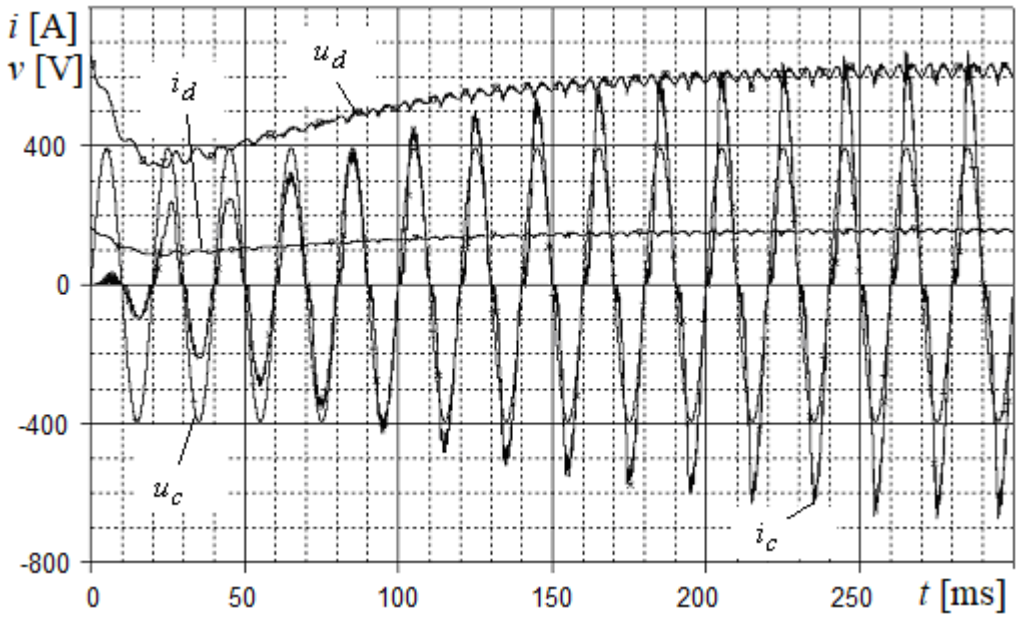

Figure 2. Results of simulation of ACPF at $R_{load\_rated} = 3.94$ Ohm, $a_i = a_v = 4$ (transient process of turning on ACPF with capacitors C_d and C_{rf} pre-charged to rated voltage $v_d = 600$ V) using a current A-controller and a voltage PI-controller.

Preprints.org (www.preprints.org) | NOT PEER-REVIEWED | Posted: 23 May 2024 doi:10.20944/preprints202405.1572.v1

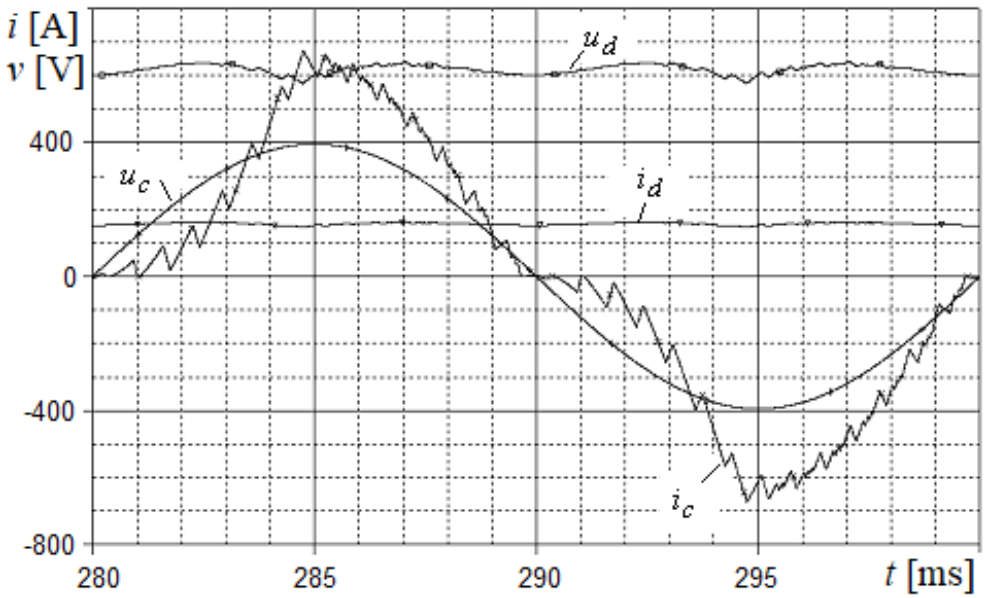

Figure 3. Simulation results of ACPF at $R_{load\_rated} = 3.94$ Ohm (steady state mode) using a current A-controller and a voltage PI-controller.

The simulation results at $R_{load} = 5 \cdot 3.94 = 19.7$ Ohm we can see in Figure 4.

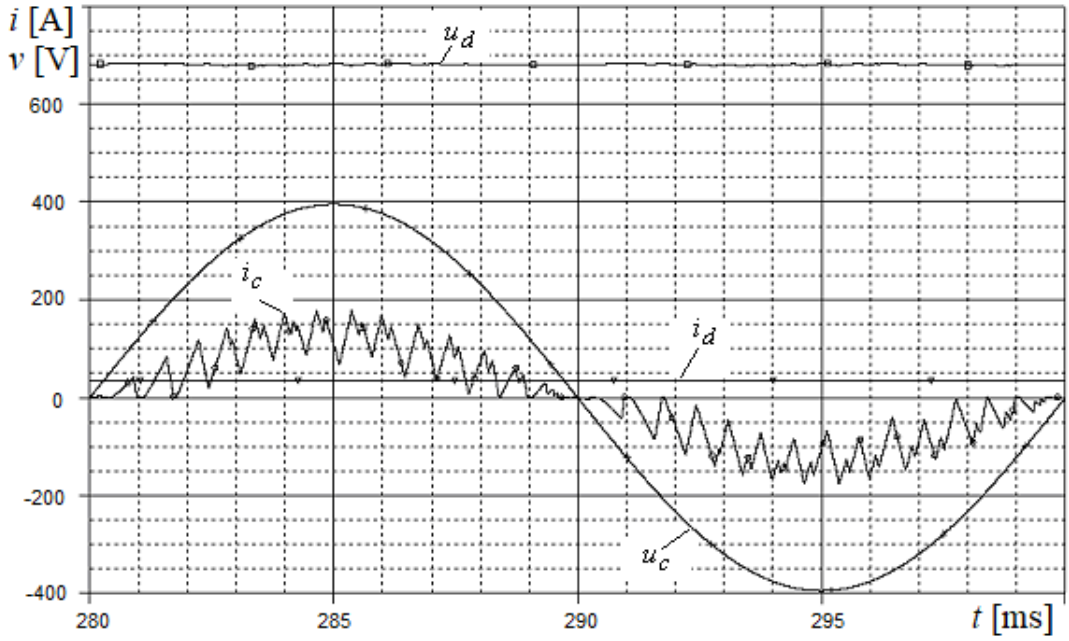

Figure 4. Simulation results of ACPF at $R_{load} = 19.7$ Ohm (steady state mode) using a current A-controller and a voltage PI-controller.

As an alternative to the above-described structure of the ACPF cascaded two loops control, a similar structure can be proposed, where instead of an aperiodic current controller a proportional one is used (P-controller). In this case, the following are accepted as prerequisites for the synthesis of the system:

$$W_{open\_desired\_i}(s) = \frac{1}{a_i \cdot T_\mu \cdot s}; \qquad (17)$$

 doi:10.20944/preprints202405.1572.v1

$$W_{open\_desired\_v}(s) = \frac{1}{a_v \cdot a_i \cdot T_\mu \cdot s}; \quad (18)$$

$$W_{ch}(s) = k_{ch}. \quad (19)$$

As a result of transformations, we obtain the TF of the current controller in the form

$$W_{controller\_i}(s) = \frac{W_{open\_drsired\_i}(s)}{k_{si} \cdot W_{plant\_i}(s)} = \frac{\frac{1}{a_i \cdot T_\mu \cdot s}}{k_{si} \cdot \frac{1}{L_1 \cdot s}} =,$$

$$= \frac{L_1}{k_{si} \cdot a_i \cdot T_\mu} = k_{controller\_i}, \quad (20)$$

and the TF of the voltage regulator in the form

$$W_{controller\_v}(s) = \frac{W_{open\_desired\_v}(s)}{k_{sv} \cdot W_{closed\_i}(s) \cdot W_{ch}(s)} = \frac{\frac{1}{a_v \cdot a_i \cdot T_\mu \cdot s}}{k_{sv} \cdot \frac{1/k_{si}}{a_i \cdot T_\mu \cdot s + 1} \cdot k_{ch}} =$$

$$= \frac{k_{si}}{a_v \cdot k_{ch} \cdot k_{sv}} \cdot \left(1 + \frac{1}{a_i \cdot T_\mu \cdot s}\right) = k_{controller\_v} \left(1 + \frac{1}{T_{controller\_v} \cdot s}\right), \quad (21)$$

where $k_{controller\_v} = \frac{k_{si}}{a_v \cdot k_{ch} \cdot k_{sv}}$ is the gain of the voltage controller; $T_{controller\_v} = a_i \cdot T_\mu$ – time constant of the voltage controller.

Simulation of an alternative control structure for the ACPF show that at rated load it gives results similar to the previous scheme (Figures 5 and 6), but in modes close to no-load (Figure 7) compared to Figure 4, the shape of the input current is significantly worsened, its amplitude increases, and v_d voltage stabilization is worse.

Preprints.org (www.preprints.org) | NOT PEER-REVIEWED | Posted: 23 May 2024 doi:10.20944/preprints202405.1572.v1

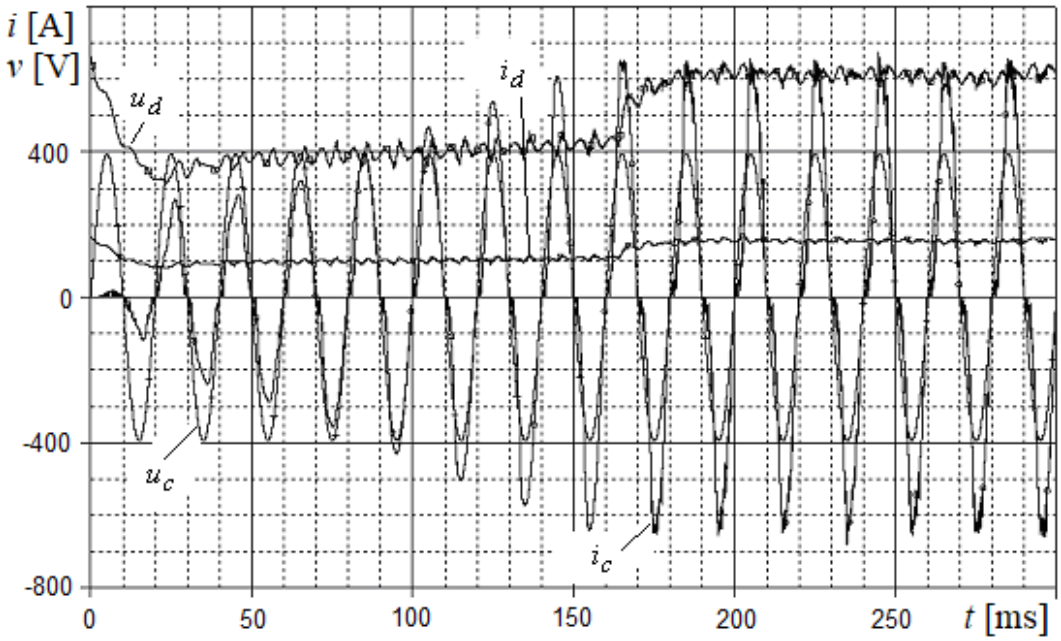

Figure 5. Results of simulation of ACPF at $R_{load\_rated} = 3.94$ Ohm, $a_i = a_v = 4$ (similar to Figure 2) using a current P-controller and a voltage PI-controller.

Comparative quantitative characteristics of the ACPF for different control structures, obtained by analyzing the results of computer simulations, are presented in the Table 1, where the basic value 660 V selected for calculating the v_d oscillation range (Figures 3, 4, 6, 7) and v_d lowest value during transient process (Figures 2, 5) 660 V selected.

Figure 8 shows simulation results similar to Figure 2, but a successful attempt was made to increase the speed of the ACPF automatic control system's response: the duration of the transition process was reduced by 10 times. For this purpose it is specified in the settings $a_i = a_v = 1$.

A possible compromise between increasing the speed of the control system's response and maintaining a close-to-sinusoidal shape of the input current in steady state modes under conditions close to no-load is the use of settings $a_i = 4; a_v = 3$.

If, all other things being equal, we take the relation $T_\mu = T_{ch}$ instead of the relationship $T_\mu = 0.1 \cdot T_{ch}$ discussed above, this leads to a slowdown in the system's response, an approximation of the shape of the AC input current to a triangular one, and an increase in the amplitude of the input current by 25%.

As stated earlier, this is usually assumed u_c to be sinusoidal. In fact, its shape is often far from ideal due to the influence of nonlinear loads. In particular, when using electric locomotives with traction rectifier-inverter converters with zone-phase control, significant non-sinusoidality of v_c is caused by switching processes inside traction converter. An example of such a distorted voltage on the auxiliary winding of the traction transformer of 2ES5K Ermak electric locomotive is given in [25]. To clarify the influence of non-sinusoidality and v_c RMS value fluctuations on the functioning of the ACPF, computer simulation was carried out when v_c represented by a polyharmonic signal. In addition to this, the RMS value of the fundamental harmonic of the input voltage changes during 20 ms (from the moment of time 50 ms) from 270 V to 470 V. The simulation results are shown in Figure 9. It can be seen that non-sinusoidality of v_c itself does not significantly worsen the shape of i_c (the first half-cycle in Figure 9). To a greater extent, the i_c shape deteriorates and becomes intermittent as v_c increases, when for v_d stabilization it is necessary to allow long pauses between the

Preprints.org (www.preprints.org) | NOT PEER-REVIEWED | Posted: 23 May 2024 doi:10.20944/preprints202405.1572.v1

conducting states of transistor VT1 when preset DC voltage level $v_{d\max} = 700$ V is exceeded, which reduces the power factor.

Table 1. Comparative characteristics of ACPF under different control system's structures, obtained as a result of computer simulations (Figures 2– 7).

Name, symbol and dimension of the characteristic	**The control system's structure of ACPF contains**	
	Current A-controller and a voltage PI-controller (Figures 2–4)	Current P-controller and a voltage PI-controller (Figures 5–7)
	Transient mode	
The transient mode duration, ms	240	180
Lowest v_d value during transient mode, %	51.5	47.5
	Steady state mode	
v_d oscillation range at rated load, %	9.5	12.5
v_d oscillation range at no-load conditions, %	2.2	5.9
Highest i_c value at rated load, A	672.5	647.1
Highest i_c value at no-load conditions, A	176.4	335.3

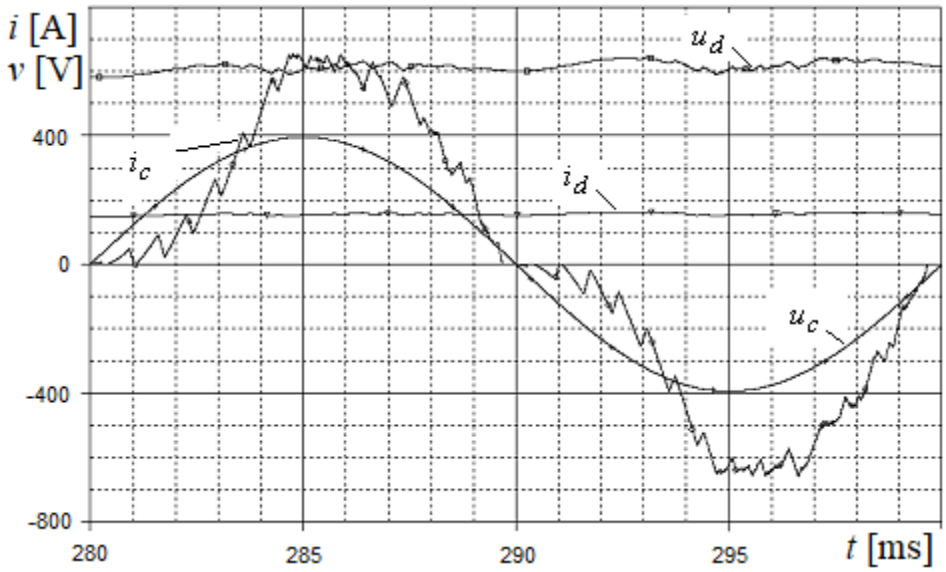

Figure 6. Simulation results of ACPF at $R_{load\_rated} = 3.94$ Ohm (steady state mode) using a current P-controller and a voltage PI-controller.

Preprints.org (www.preprints.org) | NOT PEER-REVIEWED | Posted: 23 May 2024 doi:10.20944/preprints202405.1572.v1

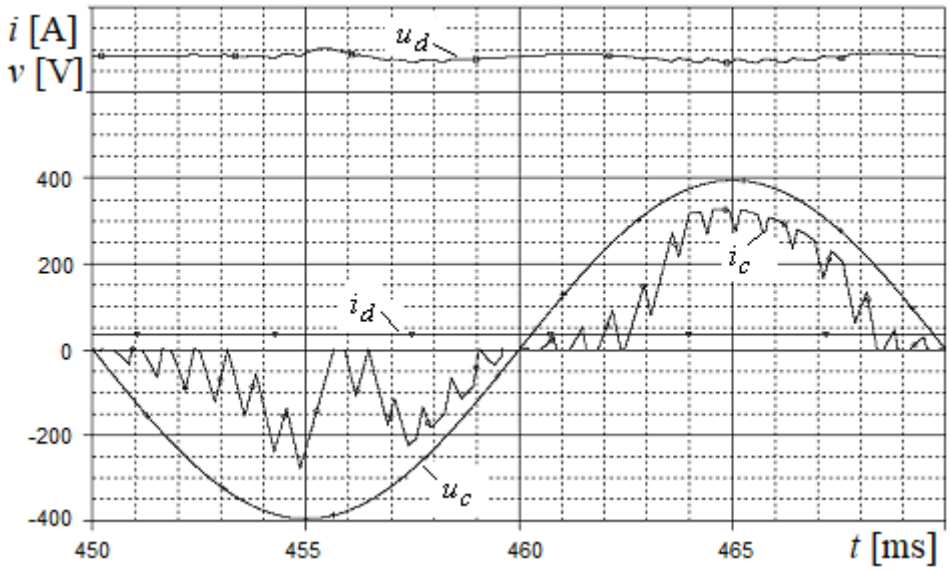

Figure 7. Simulation results of ACPF at $R_{load} = 19.7$ Ohm (steady state mode) using a current P-controller and a voltage PI-controller.

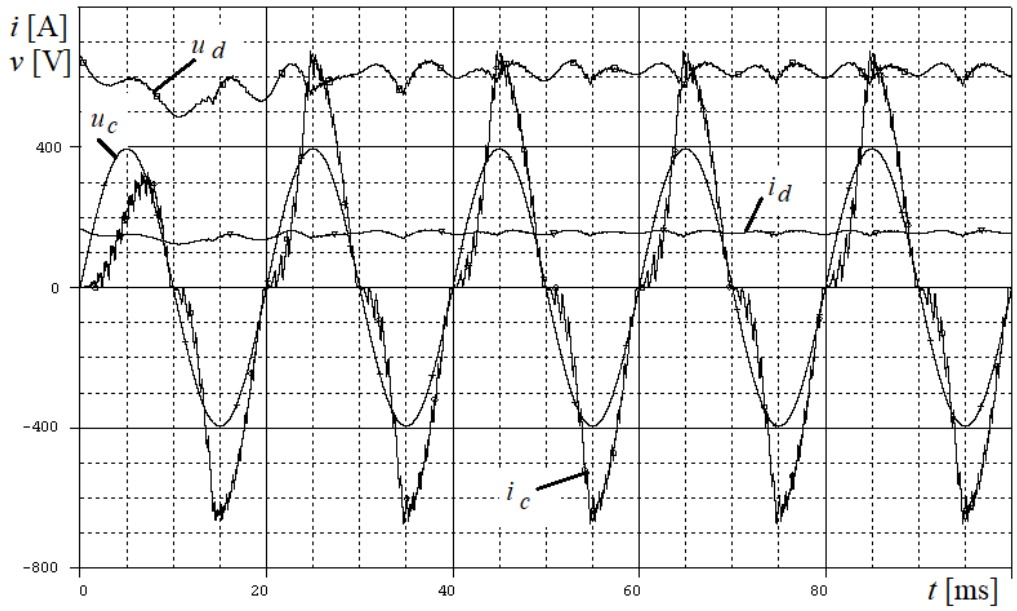

Figure 8. Results of simulation of ACPF at $R_{load\_rated} = 3.94$ Ohm, $a_i = a_v = 1$ (transient process of turning on ACPF with capacitors C_d and C_{rf} pre-charged to rated voltage $v_d = 660$ V) using a current A-controller and a voltage PI-controller.

 doi:10.20944/preprints202405.1572.v1

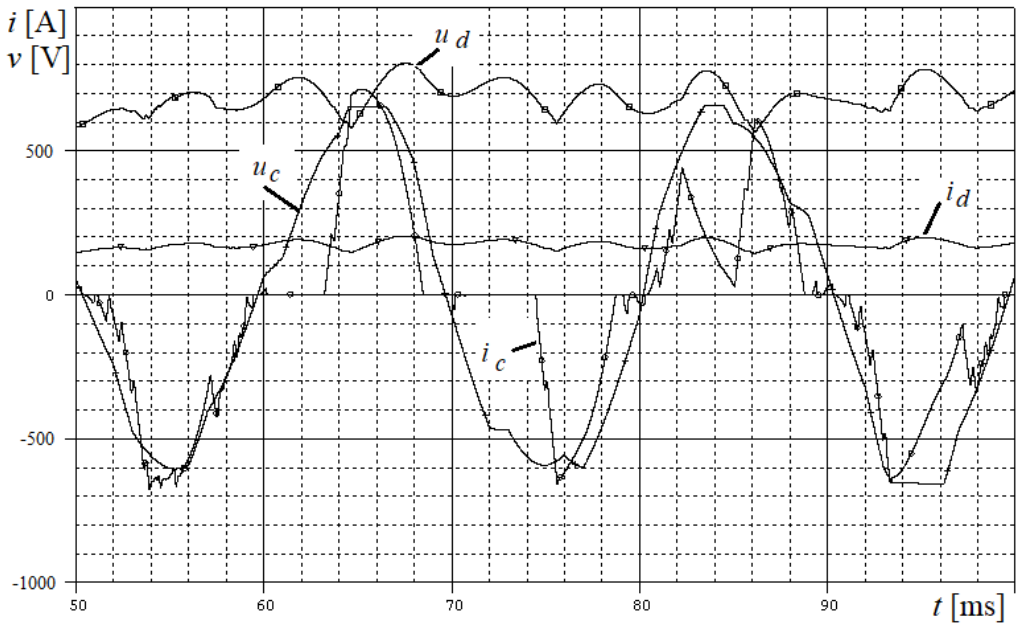

Figure 9. Fragment of the simulation results for ACPF $R_{load\_rated} = 3.94$ Ohm, $a_i = a_v = 1$, under conditions of polyharmonic input voltage varying from 270 to 470 V during 20 ms using a current A-controller and a voltage PI-controller.

4. Discussion and Conclusions

Based on the analysis of the computer simulation results, it should be recognized that a cascaded two loops control system, containing a current A-controller and a voltage PI-controller, is suitable for ACPF as part of an auxiliary electric drive of electric locomotives, since such a structure provides a smaller dynamic voltage drop when connecting a load, a smaller amplitude of DC voltage ripples on load, lower input current amplitude at no load condition and it's better sinusoidality. The choice of settings for the control system requires additional research from the point of view of achieving the best result, taking into account the speed of the system's response, the approximation of the shape of input current to sinusoidal over a wide range of load values, and in case of fluctuations of the input voltage.

Author Contributions: Conceptualization, supervision, writing—review and editing A.L.; formal analysis, investigation, writing—original draft, M.P. All authors have read and agreed to the published version of the manuscript.

Funding: This research received no external funding.

Data Availability Statement:. The original contributions presented in the study are included in the article, further inquiries can be directed to the corresponding author.

Conflicts of Interest: The authors declare no conflicts of interest.

Abbreviations

The following abbreviations are used in this manuscript:

A-controller	Aperiodic controller
AC	Alternating current
ACPF	Active corrector of power factor
CC	Current controller
CS	Rectified current sensor
DC	Direct current
LPF	Low pass filter

 doi:10.20944/preprints202405.1572.v1

NE	Nonlinear element
op-amp	Operational amplifier
P-controller	Proportional controller
PI-controller	Proportional-integral controller
PWVC	Pulse-width voltage control
RG	Ramp generator
RMS	Root mean square
SSPC	Setter of the shape (sinusoid) and phase of the AC input current
TF	Transfer function
TVG	Triangular voltage generator
VC	Voltage controller
VS	load DC voltage sensor

References

1. Pustovetov, M.Y., Voinash, S.A. Analysis of dv/dt Filter Parameters Influence on its Characteristics. Filter Simulation Features. In Proceedings of the 2019 International Conference on Industrial Engineering, Applications and Manufacturing (ICIEAM), Sochi, Russia, 25-29 March 2019, pp. 1-5. https://doi.org/10.1109/ICIEAM.2019.8743007.
2. Pastura, M., Nuzzo, S., Kohler M., Barater, D. Dv/Dt Filtering Techniques for Electric Drives: Review and Challenges. In Proceedings of the IECON 2019 - 45th Annual Conference of the IEEE Industrial Electronics Society, Lisbon, Portugal, 14-17 October 2019, pp. 7088-7093. https://doi.org/10.1109/IECON.2019.8926663.
3. Pustovetov, M.Y. The Procedure of Sine-Wave Filter Parameters Selection Including Simulation in Case of Increased Frequency of Voltage. In Proceedings of the 2020 International Multi-Conference on Industrial Engineering and Modern Technologies (FarEastCon), Vladivostok, Russia, 06-09 October 2020, pp. 1-8. https://doi.org/10.1109/FarEastCon50210.2020.9271606.
4. Baek Seunghoon; Choi Dongmin; Bu Hanyoung; Cho Younghoon. Analysis and Design of a Sine Wave Filter for GaN-Based Low-Voltage Variable Frequency Drives. *Electronics* **2020**, *Volume 9, No. 345*, 76-89. https://doi.org/10.3390/electronics9020345.
5. Pustovetov, M. Determination of the Sufficient Inductance of AC Line Reactor at the Input of Frequency Converter. *Journal of Modeling and Optimization* **2019**, *11*, 25-29. https://doi.org/10.32732/jmo.2019.11.1.25.
6. Balci, S., Altin, N., Ozdemir, S., Sefa, I. FEM based parametric analysis of AC line reactors. In Proceedings of the 4th International Conference on Power Engineering, Energy and Electrical Drives, Istanbul, Turkey, 13-17 May 2013, pp. 1328-1333. https://doi.org/10.1109/PowerEng.2013.6635806.
7. Mohan, N., Undeland, T.M., Robbins, W.P. *Power Electronics. Converters, Applications, and Design,* 3rd Ed.; John Wiley & Sons, Inc. John Wiley & Sons: Hoboken, NJ, USA, 2003; 802 p.
8. Title of Site. Available online: URL (accessed on Day Month Year).
9. Ribickis, L., Peuteman, J., Galkins, I., Raņķis, I., Vanoost, D., Žiravecka, A. *Power Electronics*; RTU Press: Riga, Latvia, 2015; 277 p.
10. Sujata Powniker, Sachin Shelar. Development of Active Power Factor Correction controller using boost converter. In Proceedings of the 2016 IEEE International WIE Conference on Electrical and Computer Engineering (WIECON-ECE), Pune, India, 19-21 December 2016, pp. 212-216. https://doi.org/10.1109/WIECON-ECE.2016.8009120.
11. Sujata Nazarkar, Sachin Shelar. Design & Simulation of Active Power Factor Controller Using Boost Converter. *Novateur Publications International Journal of Innovations in Engineering Research and Technology (IJIERT)* **2016**, *3*, 1-8.
12. Glyzin, I.I.; Inkov, Y.M.; Kuchumov, V.A.; Litovchenko, V.V. Improving the Energy Efficiency of a Traction Network and Electric Rolling Stock of Alternating Current with a 4qs-Converter. *Russ. Electr. Engin.* **2019**, *90*, 641-646. https://doi.org/10.3103/S1068371219090050.
13. In'kov, Y.M.; Litovchenko, V.V.; Feoktistov, V.P. A Two-System Freight Electric Locomotive for Railroads of the Russian Federation. *Russ. Electr. Engin.* **2014**, *85*, 176-182. https://doi.org/10.3103/S1068371214030079.
14. Fedotov, Y.B., Tishkin, A.A., Kurganov, A.A., Bobrov, M.A. Research of Three-Phase Rectifier with Active Power Factor Corrector. In Proceedings of the XIV International Scientific-Technical Conference on Actual Problems of Electronics Instrument Engineering (APEIE), Novosibirsk, Russia, 02-06 October 2018, pp. 103-107. https://doi.org/10.1109/APEIE.2018.8546234.

15. He, L., Xiong, J., Ouyang, H., Zhang, P., Zhang, K. *High-Performance Indirect Current Control Scheme for Railway Traction Four-Quadrant Converters*. *IEEE Transactions on Industrial Electronics*. **2014,** *Volume 61, No. 12,* 6645-6654. https://doi: 10.1109/TIE.2014.2316240.
16. Alotaibi, S., Darwish, A., Ma X., Williams, B.W. A New Four-Quadrant Inverter Based on Dual-Winding Isolated Cuk Converters for Railway and Renewable Energy Applications. In Proceedings of the 10th International Conference on Power Electronics, Machines and Drives (PEMD 2020), Online Conference, 15-17 December 2020, pp. 926-931. https://doi: 10.1049/icp.2021.1033.
17. Xu, D., Zhang, G., Hao, F., Hu, Z. (2018). The LCL Filtering Scheme of High Power Four-Quadrant Converter Used in Urban Rail Transit. In: Jia, L., Qin, Y., Suo, J., Feng, J., Diao, L., An, M. (eds) Proceedings of the 3rd International Conference on Electrical and Information Technologies for Rail Transportation (EITRT) 2017. EITRT 2017. Lecture Notes in Electrical Engineering, Volume 482. Springer, Singapore. https://doi.org/10.1007/978-981-10-7986-3_57.
18. Pustovetov, M. Refined Computer Model of Auxiliary Induction Motor of Electric Locomotive Powered by Autonomous Voltage Inverter. *DS Journal of Modeling and Simulation*, **2023**, *Volume 1, No. 1*, 9-24. https://doi.org/10.59232/MS-V1I1P102.
19. Wildi, T. *Electrical Machines, Drives, and Power Systems*. 5th Ed.; Prentice Hall: Upper Saddle River, USA, 2002; 886 p.
20. Wescott, T. *Applied Control Theory for Embedded Systems*. Elsevier: Amsterdam, Netherlands, 2006; 320 p.
21. Larsson, T., Skogestad, S. Plantwide Control - a Review and a New Design Procedure. *Modeling, identification and control*. **2000,** *Volume 21, No. 4,* 209–240. https://doi:10.4173/mic.2000.4.2.
22. Klyuchev, V.I. *Electric Drive Theory: textbook for universities*. 2nd Ed.; Energoatomizdat: Moscow, Russia, 2001; 704 p.
23. Golnaraghi, F., Kuo, B.C. *Automatic Control Systems*. 10th Ed.; McGraw-Hill: New York, USA, 2017; 944 p.
24. Onishchenko, G.B. *Electric Drive: a textbook for universities*. RASHN: Moscow, Russia, 2003; 320 p.
25. Pustovetov, M.Yu., Pustovetov, K.M. The Electromagnetic Torque Ripple of Three-Phase Induction Electric Machine, Operating as a Part of the Auxiliary Electric Drive Onboard of AC Electric Locomotive - a Factor Contributing to the Failure of Bearings. In Proceedings of the 2018 International Multi-Conference on Industrial Engineering and Modern Technologies (FarEastCon), Vladivostok, Russia, 03-04 October 2018, pp. 1-4. https://doi.org/10.1109/FarEastCon.2018.8602672.